

Model for frustrated spin-orbital chains: application to CaV_2O_4

Gia-Wei Chern¹ and Natalia Perkins¹

¹*Department of Physics, University of Wisconsin, Madison, Wisconsin 53706, USA*

(Dated: October 28, 2018)

Motivated by recent interest in quasi-one-dimensional compound CaV_2O_4 , we study the ground states of a spin-orbital chain characterized by an Ising-like orbital Hamiltonian and frustrated interactions between $S = 1$ spins. The on-site spin-orbit interaction and Jahn-Teller effect compete with inter-site superexchange leading to a rich phase diagram in which an antiferro-orbital phase is separated from the orbital paramagnet by a continuous Ising transition. Two distinct spin liquids depending on the underlying orbital order are found in the limit of small spin-orbit coupling. In the opposite limit, the zigzag chain behaves as a spin-2 chain with Ising anisotropy. The implications for CaV_2O_4 are discussed.

Orbital degrees of freedom have been shown to play an important role in understanding the electronic and magnetic properties of transition metal oxides.¹ This is particularly so for frustrated magnets with partially filled orbitals. A well-studied case is vanadium spinels AV_2O_4 where the A -site sublattice is occupied by divalent ions such as Zn^{2+} or Mn^{2+} , and the B -site magnetic V^{3+} ions form a *pyrochlore* lattice.^{2,3} It is known that geometrical frustration of classical spins on such a lattice precludes simple Néel ordering and gives rise to a highly degenerate ground state. Orbital ordering in these compounds partially relieves the frustration by creating disparities in nearest-neighbor exchange constant, hence setting the stage for magnetic ordering at lower temperatures.^{4,5}

In this paper, we investigate the physics of frustrated vanadium chains in which the interplay of geometrical frustration, spin-orbital couplings, Jahn-Teller effect, and enhanced quantum fluctuations leads to a rich phase diagram. Our work is partly motivated by an attempt to understand another vanadium compound CaV_2O_4 , which at room temperature crystallizes in the orthorhombic calcium-ferrite structure (space group $Pnam$).^{6,7,8,9,10} Contrary to its spinel cousins, V^{3+} ions in CaV_2O_4 are arranged in zigzag chains of edge-sharing VO_6 octahedra (Fig. 1). Antiferromagnetic interaction on zigzag chains consisting of triangular loops is subject to geometrical frustration as well. The rather weak and frustrated inter-chain couplings make the vanadium chains quasi-1D systems susceptible to quantum fluctuations. Couplings of vanadium orbitals to spins and phonons add yet another dimension to the intriguing physics of zigzag chains.

In CaV_2O_4 , the zigzag geometry results in a spin-1 chain with comparable nearest and next nearest-neighbor interactions. Combined with the observation that $3d^2$ configuration of V^{3+} ions tend to have an easy-plane anisotropy,¹⁰ the quasi-1D compound CaV_2O_4 has been a favorable candidate for the long-sought chiral spin liquid where a long-range chiral order coexists with algebraically decaying spin correlations.^{10,11} However, as first pointed out by Pieper *et al.*,⁸ orbital degeneracy in this compound drastically changes the above picture. Since the t_{2g} levels are split into a singlet and a doublet due to a flattened VO_6 octahedron, with the low-energy singlet

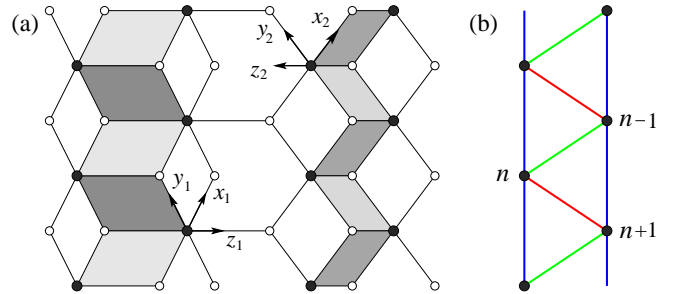


FIG. 1: (Color online) (a) Two crystallographically inequivalent vanadium chains in CaV_2O_4 . The V^{3+} ions are arranged in zigzag chains of edge-sharing VO_6 octahedra. For both vanadium sites, the VO_6 octahedra is flattened at room temperatures. A local reference frame is defined in such a way that z -axis is parallel to the tetragonal axis of the crystal field. The black and white circles denote the vanadium and oxygen ions, respectively. (b) A simplified view of the zigzag chain. The red, green, and blue bonds are parallel to the local $[011]$, $[110]$ and $[101]$ axes, respectively. Consequently, electron hopping on the red, green, and blue bonds is possible only when d_{yz} , d_{zx} and d_{xy} orbitals are occupied, respectively.

always occupied, a double degeneracy remains for the other electron. The orbital degrees of freedom in V^{3+} ion is thus described by an Ising-like variable.

Recent experimental studies on CaV_2O_4 seem to rule out a possible chiral liquid phase as well. A structural transition at $T_s \approx 141$ K reduces the crystal symmetry to monoclinic $P2_1/n$.^{8,9} It was suggested in Ref. 8 that the simultaneous orbital ordering relieves the magnetic frustration of zigzag chains. As the inter-chain frustration is also lifted by the lattice distortion, a three-dimensional Néel order sets in at $T_N \approx 71$ K. The collinear spins are parallel to the crystal b -axis as evidenced by both nuclear magnetic resonance and neutron diffraction measurements.^{6,7,8}

To make progress toward an understanding of the ground-state structure and the nature of phase transitions in CaV_2O_4 , here we study the zero-temperature phase diagram of its building blocks, i.e. zigzag chains with $S = 1$ spins and Ising orbital variables. We propose a theoretical model which includes the superex-

change (SE) interaction, relativistic spin-orbit (SO) coupling, and Jahn-Teller (JT) effect. We find that antiferro-orbital order favored by an Ising-like orbital exchange is destroyed in the presence of large on-site spin-orbit or Jahn-Teller coupling. Depending on the underlying orbital configuration, magnetic properties of the zigzag chain is equivalent either to those of two weakly coupled $S = 1$ chains, or of an unfrustrated spin-1 ladder. In the limit of large spin-orbit coupling, the zigzag chain can be viewed as a spin-2 chain with anisotropic interaction. Finally, we discuss implications for CaV_2O_4 .

Model Hamiltonian. We first define a local reference frame for the two crystallographically inequivalent vanadium chains (referred to as type-I and II chains here) in CaV_2O_4 such that the z -axis is parallel to the tetragonal direction of flattened VO_6 octahedron [Fig. 1(a)]. Nearest-neighbor bonds along the chain are parallel to the local [011] and [101] directions alternatively. In the following, we employ a convention in which even-numbered bonds are along the [011] axis.

Geometrical frustration of the zigzag chain comes from the fact that second-nearest-neighbor bonds parallel to local [110] axis have a length close to that of nearest-neighbor bonds. In fact, the second-nearest-neighbor interaction is the dominant one as d_{xy} orbital is occupied at every site due to the flattened VO_6 octahedra. The remaining orbital degeneracy is described by a pseudospin- $\frac{1}{2}$ with $\sigma^z = \pm 1$ corresponding to the $|yz\rangle$ and $|zx\rangle$ states, respectively.

Having introduced the basic notations, we now discuss a minimal model for the spin-orbital chain. Since orbital interaction with a 90° angle between vanadium-oxygen bonds is governed by direct $dd\sigma$ exchange of t_{2g} orbitals, the corresponding spin interaction on a bond depends on whether the relevant orbital is occupied.¹² Essentially, orbitals participate in the superexchange only via orbital projectors $P_{yz/zx}$. Noting that $P_{yz/zx} = (1 \pm \sigma^z)/2$, we first define the antiferro-orbital and ferro-orbital bond operators

$$\mathcal{O}_{n,n+1} = \frac{1}{2}(1 - \sigma_n^z \sigma_{n+1}^z), \quad \bar{\mathcal{O}}_{n,n+1} = \frac{1}{4}(1 \pm \sigma_n^z)(1 \pm \sigma_{n+1}^z)$$

with \pm signs for even and odd numbered bonds, respectively. The model Hamiltonian is divided into three parts: $H = H_0 + H_\perp + H_{\text{on-site}}$. The first H_0 term represents decoupled spin and orbital systems

$$H_0 = J_2 \sum_n \mathbf{S}_n \cdot \mathbf{S}_{n+2} - \sum_n (K \mathcal{O}_{n,n+1} + K' \bar{\mathcal{O}}_{n,n+1}). \quad (1)$$

Since J_2 couples every second-nearest neighbors, the spin part can be viewed as two decoupled $S = 1$ Haldane chains, corresponding to the two blue lines in Fig. 1(b). The K and K' terms denote the energy gain of an antiferro-orbital and a ferro-orbital bond, respectively. In general, we have $K > K'$ due to a finite on-site Hund's coupling J_H , hence an antiferro-orbital order in the ground state of H_0 .

The H_\perp term introduces interactions between the two spin-1 chains:

$$H_\perp = \sum_n (J_1 \bar{\mathcal{O}}_{n,n+1} - J'_1 \mathcal{O}_{n,n+1}) \mathbf{S}_n \cdot \mathbf{S}_{n+1}. \quad (2)$$

As discussed above interaction between spins depends on orbital occupations: the antiferromagnetic coupling J_1 is nonzero only when d_{yz} (d_{zx}) orbital is occupied at both sites of an even (odd) bond, whereas the strength of ferromagnetic J'_1 term depends on the expectation value of the antiferro-orbital bond operator $\mathcal{O}_{n,n+1}$.

Explicit expressions relating the exchange constants to microscopic parameters are obtained from the SE Hamiltonian of vanadium spinels,¹² where neighboring VO_6 octahedra share the same edge as in zigzag chains considered here. Assuming an exact octahedral site-symmetry, we find $K = (1 + 2\eta) \frac{t^2}{U}$, $J_2 = J_1 = K' = (1 - \eta) \frac{t^2}{U}$, and $J'_1 = \eta \frac{t^2}{U}$ to lowest order in Hund's parameter $\eta \equiv J_H/U$. Here t is the hopping integral, and U is the on-site Coulomb repulsion. The parameters of the model can be estimated from known values of the same parameters in other vanadium compounds. Measurements on cubic vanadates yield $J_H \simeq 0.68$ eV, $U \simeq 6$ eV, and $t \simeq -0.35$ eV,^{13,14} which gives $\eta \simeq 0.11$ and $t^2/U \simeq 20.4$ meV. The estimate of λ is less certain, we find $\lambda \simeq 13 - 25$ meV.^{5,13,15,16} In the following, we shall measure energy in units of t^2/U .

The remaining single-ion interactions are included in the Hamiltonian

$$H_{\text{on-site}} = -\lambda \sum_n \sigma_n^x S_n^z - \delta \sum_n \sigma_n^z. \quad (3)$$

The first term originates from relativistic SO coupling $\lambda(\mathbf{L} \cdot \mathbf{S})$. Since d_{xy} orbital is always occupied, the x and y components of the orbital angular momentum are quenched; the remaining $L^z = -\sigma^x$ in the pseudospin representation. A similar situation has been studied in cubic vanadates.¹⁷ The effect of the monoclinic structural transition at T_s is modeled by the second term with 2δ denoting the level splitting due to the induced orthorhombic distortion of VO_6 octahedra. Note that the orthorhombic distortion is different on type-I and II chains.^{8,9}

Orbital orders. We first consider a simpler case of the model Hamiltonian by assuming the presence of a collinear Néel order on the zigzag chain. This is a plausible assumption as the SO term $\lambda \sigma_n^x S_n^z$ breaks the spin $\text{SU}(2)$ symmetry and, as will be discussed later, closes the energy gap of longitudinal magnons at large enough λ , hence signaling a transition to the Néel state with S_n^z parallel to $\pm \hat{z}$. Even with this simplification, the competition between inter-site exchange and various on-site interactions still poses a rather nontrivial problem. This study also sheds light on orbital orders in the ground state of CaV_2O_4 , where spins develop a three-dimensional collinear antiferromagnetic order at $T_N \approx 71$ K.

Due to the strong second nearest-neighbor exchange J_2 , collinear orders on a zigzag chain consisting of repeated $+-$ spins have a quadrupled unit cell. There

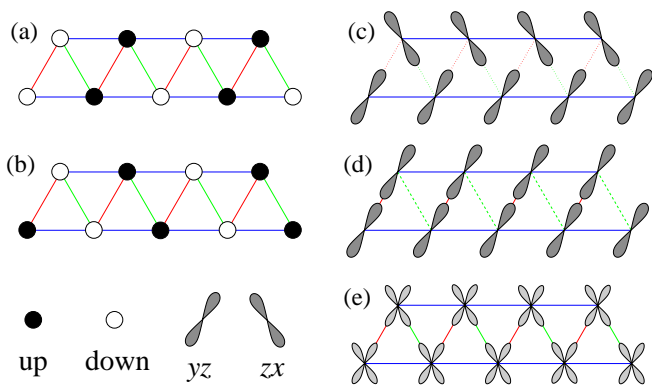


FIG. 2: (Color online) Spin and orbital orders on a zigzag vanadium chain. Néel orders (a) and (b) are related to each other by lattice translations. There are a total of four degenerate Néel states; the other two are related to states (a) and (b) by time reversal. (c) antiferro-orbital order consisting of staggered d_{yz} and d_{zx} orbitals. (d) and (e) correspond to ferro-orbital orders with real orbital d_{yz} and complex orbitals $(d_{yz} \pm id_{zx})/\sqrt{2}$, respectively.

are a total of four degenerate Néel states related to each other by lattice translations and time reversal [Figs. 2(a) and (b)]. After applying a π -rotation about z -axis to pseudospins at $S_n^z < 0$ sites, we obtain an effective orbital Hamiltonian:

$$H_{\text{orb}} = \sum_n [\mathcal{J} + (-1)^n \mathcal{K}] \sigma_n^z \sigma_{n+1}^z - \sum_n (h_z \sigma_n^z + h_x \sigma_n^x). \quad (4)$$

This model is equivalent to an Ising chain with alternating nearest-neighbor couplings in a skewed magnetic field. The effective exchange constants are $\mathcal{J} = (2K - K')/4$ and $\mathcal{K} = \nu^2(2J'_1 + J_1)/4$. Here we have assumed $\langle \mathbf{S}_n \cdot \mathbf{S}_{n+1} \rangle = \mp \nu^2$ on even and odd bonds, respectively. The longitudinal and transverse fields are given by $h_z = \delta + \nu^2 J_1/2$ and $h_x = \lambda$, respectively. The parameter $\nu < 1$ characterizes the magnitude of the Néel order. Its value can only be determined with a proper treatment of the SO coupling term. For simplicity, we set $\nu = 1$ in the following calculation. Hamiltonian (4) without the staggered exchange \mathcal{K} is one of the simplest models exhibiting nontrivial quantum critical point:¹⁸ numerical calculation shows an order-disorder transition belonging to 2D Ising universality class. The staggered exchange \mathcal{K} involves higher-order spatial derivatives in the continuum limit and thus represents an irrelevant perturbation in the RG sense.

A schematic phase diagram of model (4) is shown in Fig. 3(a), where an antiferro-orbital phase is separated from the orbital paramagnet by an Ising transition line. Along the δ -axis ($\lambda = 0$), the antiferro-orbital phase coexists with ferro-orbitally ordered phase, shown in Figs. 2(c) and (d) respectively, at the multicritical point $\delta_c = (2K - K' - J_1)/2$. On the other hand, in the large λ limit, the pseudospins are polarized by the transverse field h_x such that spins $S^z = \pm 1$ are accompanied

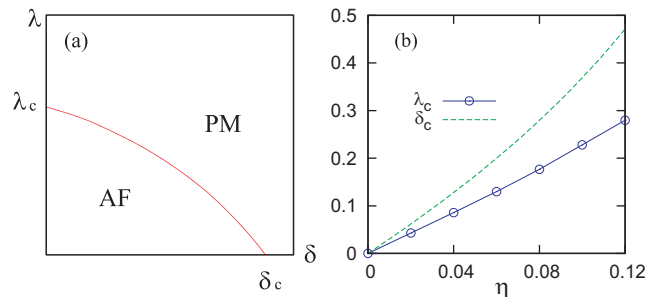


FIG. 3: (a) Schematic phase diagram of orbitals in the presence of a collinear Néel order on the zigzag chain, effectively described by Hamiltonian (4). AF and PM refer to antiferro-orbitally ordered and orbital paramagnetic phases, respectively. (b) Critical boundaries λ_c and δ_c measured in units of t^2/U versus Hund's parameter η . The critical distortion is determined analytically from $\delta_c = (2K - K' - J_1)/2$, whereas λ_c is obtained from DMRG calculation. The various effective parameters in Eq. (4) are expressible in terms of model parameters J_1 , J'_1 , J_2 , K , and K' of the original SE Hamiltonian, whose relations to η and t^2/U can be found in the text.

by complex orbitals $\frac{1}{\sqrt{2}}(d_{yz} \pm id_{zx})$, respectively, resulting in a uniform orbital occupation $n_{yz} = n_{zx} = 1/2$ at all sites [Fig. 2(e)]. Using the infinite-system DMRG method with periodic boundary condition,¹⁹ we obtain a critical λ_c at $\delta = 0$, taking into account the effect of staggered \mathcal{K} . The Ising transition line is bounded by the critical points $(\delta_c, 0)$ and $(0, \lambda_c)$. Fig. 3(b) shows δ_c and λ_c as a function of parameter $\eta = J_H/U$. As expected, the antiferro-orbital phase shrinks with decreasing Hund's coupling J_H . In a full quantum treatment of the zigzag chain, we expect a similar critical line characterized by massless orbital excitations (Fig. 4).

Spin liquid phases. We now discuss the original Hamiltonian (1)–(3) in small λ limit without assuming the existence of a magnetic order. It is important to note that the spin part of the Hamiltonian in this limit preserves a continuous SU(2) symmetry, which can not be broken in one dimension. One thus expects stable spin-liquid phases whose properties depend critically on orbital configurations. Furthermore, the absence of σ^x term at $\lambda = 0$ indicates that the orbital part is described by a classical Ising-like Hamiltonian. Consequently, the search of ground states reduces to first enumerate over all possible Ising configurations $\{\sigma_n^z\}$, and then compare their energies taking into account contribution from spins. As antiferro-orbital and ferro-orbital orders are favored by SE and JT interactions, respectively, it is natural to consider these two configurations first.

In the case of antiferro-orbital order [Fig. 2(c)] where bond operators $\langle \bar{\mathcal{O}}_{n,n+1} \rangle = 0$ and $\langle \mathcal{O}_{n,n+1} \rangle = 1$, the zigzag chain behaves as two spin-1 chains weakly coupled by a frustrated ferromagnetic J'_1 . The corresponding spin liquid phase (SL1 phase in Fig. 4) has an energy gap at an incommensurate wavevector.²⁰ On the other hand, the frustrated J'_1 coupling is quenched by the ferro-orbital

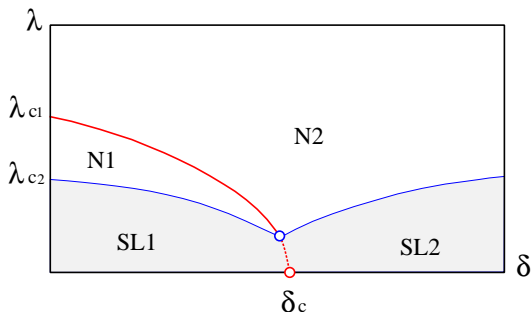


FIG. 4: (Color online) Schematic phase diagram of the zigzag vanadium chain. The various phases are characterized by the magnetic properties. SL and N represent spin liquid phase and Néel order, respectively. The SL1 and N1 phases are accompanied by an antiferro-orbital order, while in the N2 and SL2 phases the orbitals behave as an orbital paramagnet. The first-order transition along the dashed line is an extension of the multicritical point $(\delta_c, 0)$ in the phase diagram Fig. 3.

order shown in Fig. 2(d). Depending on the sign of ferro-Ising order $\langle \sigma_n^z \rangle = \pm 1$, the J_1 term is nonzero only on even or odd bonds, but not both. The spin Hamiltonian is equivalent to that of a spin-1 ladder with rung coupling J_1 . The magnetic ground state is again disordered (SL2 phase in Fig. 4).^{21,22} The magnetic energy of spin-1 ladder with arbitrary rung coupling has been calculated using quantum Monte Carlo method in Ref. 21. Comparing the energy of the two phases, including both spin and orbital contributions, yields a boundary δ_c surprisingly close to the one obtained assuming a preexisting Néel order.

Although the SU(2) symmetry is broken in the presence of SO coupling, both spin liquids persist up to finite λ . For SL2 phase stable at $\delta > \delta_c$, SO coupling provides an easy-axis anisotropy DS_z^2 with $D \simeq -\lambda^2/2\delta$. The spin-1 ladder undergoes an Ising transition to a Néel phase (N2 phase in Fig. 4) with increasing λ . At large δ , the condition $D = D_c$ gives rise to a critical $\lambda_c \propto \sqrt{\delta}$. On the other hand, Néel transition at small δ can be understood by considering the λ dependence of the spin gap in SL1 phase. The singlet ground state of weakly coupled Haldane chains has triply degenerate magnon excitations with dispersion $\omega_k = \sqrt{\Delta_0^2 + v^2(k - k_0)^2}$. In the limit of vanishing J_1' , the system reduces to two decoupled Haldane chains with $k_0 = \pi$, $\Delta_0 = 0.410J_2$ (Haldane gap for spin-1), and $v = 2.49J_2$.²³ A simple second-order perturbation calculation adds a correction to the spin gap

$$\Delta = \Delta_0 - \frac{\lambda^2 |\langle 0 | S_n^z | k_0 \rangle|^2}{\Delta_\sigma - \Delta_0}, \quad (5)$$

where $\Delta_\sigma \approx 2(\delta_c - \delta)$ is the energy of a domain-wall pair (a flipped pseudospin in the antiferro-orbital state), $|0\rangle$ is the singlet ground state, and $|k\rangle$ denotes one-magnon excitation with wavevector k . The matrix element $\langle 0 | S_n^z | k \rangle = \sqrt{Z} e^{ikn}$, with $Z \approx 1$.²³ For $\Delta_\sigma > \Delta_0$, the spin gap decreases with increasing λ and eventually

reaches zero at $\lambda_{c2} \propto \sqrt{2(\delta_c - \delta) - \Delta_0}$, signaling a transition into magnetically ordered phase (N1 phase).

The two Néel phases in Fig. 4 are distinguished by the underlying orbital orders, the phase boundary λ_{c1} separating N1 from N2 phases is thus analogous to the Ising transition line of the orbital only model [Fig. 3(b)]. Since the upper critical $\lambda_{c1} \propto J_H$, at small Hund's coupling the zigzag chain could bypass the N1 phase and enter the orbital paramagnetic phase simultaneously with a magnetic ordering. A conjectured phase diagram of the zigzag chain is shown in Fig. 4.

Anisotropic $J = 2$ spin chain. In the limit of large SO coupling, the appropriate degrees of freedom are effective spins of length $J = 2$, where $\mathbf{J} = \mathbf{L}' + \mathbf{S}$ and $L' = 1$ is the angular momentum of the unoccupied t_{2g} hole. The system thus behaves as a spin-2 chain with anisotropic exchange interaction.⁵ Furthermore, JT coupling adds an anisotropy $DJ_z^2 + E(J_x^2 - J_y^2)$, where $D < 0$ and $E \propto \delta$ are proportional to the tetragonal and orthorhombic distortions of VO₆ octahedron, respectively. Assuming a dominating easy-axis anisotropy $|D| \gg E$, the N2 phase can also be viewed as Néel ordering of the effective spins $J_z = \pm 2$ in such a way that spins of a given direction $S_z = \pm 1$ is coupled to orbital angular momenta $L'_z = \pm 1$, respectively. The corresponding ferro-orbital order with complex orbitals $d_{yz} \pm id_{zx}$ is shown in Fig. 2(e). The V³⁺ ions have a reduced magnetic moment $\mu = (2S - L')\mu_B = 1\mu_B$.

Discussion. We have presented and analyzed a minimal model of frustrated vanadium chains, pertinent to quasi-1D compound CaV₂O₄. A conjectured phase diagram (Fig. 4) is obtained based on analytical arguments and numerical calculations. The observed $P2_1/n$ crystal symmetry of CaV₂O₄ at low temperatures indicates that only *two* inequivalent vanadium sites exist as in the high temperature phase. The absence of doubled unit cell resulting from the antiferro-orbital order thus implies that both vanadium chains are in the orbital paramagnetic phase. This is a plausible conclusion noting that a rather small $\lambda_{c1} \approx 0.22(t^2/U) \approx 4.5$ meV is estimated from Fig. 3 assuming $\eta \approx 0.11$. However, the monoclinic distortion below T_s places the two types of vanadium chain at rather distinct regions of the phase diagram.

The type-I chain acquires a small δ in addition to the dominating tetragonal crystal field and behaves as a spin-2 chain subject to an easy-axis anisotropy. This Ising anisotropy is important to the stabilization of three-dimensional Néel order in CaV₂O₄, as the collinear spins are found to point along the easy axis of type-I chains.⁸ The measured V moment $1.06\mu_B$ is also consistent with the picture of an anisotropic spin-2 chain.⁷ On the other hand, a strong orthorhombic distortion δ at type-II ions completely removes the orbital degeneracy and makes the vanadium chains effectively spin-1 ladders. In fact, the well separated t_{2g} levels at type-II ions lead to a possible easy-plane spin anisotropy.⁸ Consequently, induced collinear order on type-II chains follows the spin direction of type-I vanadium ions, as indeed observed in CaV₂O₄.

Acknowledgement. We acknowledge fruitful discussions with A. Chubukov, D. Johnston, G. Japaridze, O.

Kolezhuk, B. Lake, O. Pieper and O. Tchernyshyov.

-
- ¹ M. Imada, A. Fujimori, and Y. Tokura, *Rev. Mod. Phys.* **70**, 1039 (1998).
² S.-H. Lee *et al.*, *Phys. Rev. Lett.* **93**, 156407 (2004).
³ V. O. Garlea *et al.*, *Phys. Rev. Lett.* **100**, 066404 (2008).
⁴ H. Tsunetsugu and Y. Motome, *Phys. Rev. B* **68**, 060405(R) (2003).
⁵ O. Tchernyshyov, *Phys. Rev. Lett.* **93**, 157206 (2004).
⁶ J. Hastings *et al.*, *J. Phys. Chem. Solids* **28**, 1089 (1967).
⁷ X. Zong *et al.*, *Phys. Rev. B* **77**, 014412 (2008).
⁸ O. Pieper *et al.*, *Phys. Rev. B* **79**, 180409(R) (2009).
⁹ A. Niazi *et al.*, *Phys. Rev. B* **79**, 104432(2009).
¹⁰ H. Kikuchi, M. Chiba, and T. Kubo, *Can. J. Phys.* **79**, 1551 (2001).
¹¹ T. Hikihara *et al.*, *J. Phys. Soc. Jpn.* **69**, 259 (2000).
¹² S. Di Matteo, G. Jackeli, and N. B. Perkins, *Phys. Rev. B* **72**, 020408(R) (2005).
¹³ T. Mizokawa and A. Fujimori, *Phys. Rev. B* **54**, 5368 (1996).
¹⁴ K. Takubo *et al.*, *Phys. Rev. B* **74**, 155103 (2006).
¹⁵ A. Abragam, and B. Bleaney, *Introduction to ligand field theory*, Clarendon Press - Oxford, pages 377-378 and 426-429 (1970).
¹⁶ A. Tanaka, *J. Phys. Soc. Jpn.* **71**, 1091 (2002).
¹⁷ P. Horsch, G. Khaliullin, and A.M. Oleś, *Phys. Rev. Lett.* **91**, 257203 (2003).
¹⁸ A. A. Ovchinnikov, D. V. Dmitriev, V. Ya. Krivnov, and V. O. Chervanovskii, *Phys. Rev. B* **68**, 214406 (2003).
¹⁹ S. R. White, *Phys. Rev. B* **48**, 10345 (1993).
²⁰ D. Allen and D. Sénéchal, *Phys. Rev. B* **61**, 12134 (2000).
²¹ D. Sénéchal, *Phys. Rev. B* **52**, 15319 (1995).
²² S. Todo *et al.*, *Phys. Rev. B* **64**, 224412 (2001).
²³ I. Affleck and R. Weston, *Phys. Rev. B* **45**, 4667 (1992).